ELSEVIER

Journal of Power Sources 108 (2002) 86–96

JOURNAL OF POWER SOURCES

www.elsevier.com/locate/jpowsour

Effect of heat-treatment and additives on the particles and carbon fibers as anodes for lithium-ion batteries

Gabrielle Nadeau[a], Xiang Yun Song[b], Monique Massé[a], Abdelbast Guerfi[a], Gessie Brisard[a,c], Kimio Kinoshita[b], Karim Zaghib[a,*]

[a] *Institut de Recherche d'Hydro-Québec, Service Chimie des Materiaux, 1800 boul, Lionel-Boulet, Montée Ste-Julie, Varennes, Que., Canada J3X 1S1*
[b] *Environmental Energy Technologies Division, Lawrence Berkeley National Laboratory, Berkeley, CA 94720, USA*
[c] *Department de chimie, 2500 Boul. Universite, Sherbrooke, P.Qc, Canada, J1K 2R1*

Received 8 November 2001; accepted 15 December 2001

Abstract

Carbon fiber (CF) and mesocarbon microbead (MCMB) precursors were heat-treated at 700–2800 °C, and the electrochemical and physical properties of the carbons were investigated. These carbons are quite different from natural graphite, which has a well-ordered layer planes where intercalation occur and two distinct surface sites, i.e. basal and edge plane sites. In the case of the fibers, intercalation occur by a single plane (circular area) or by two planes, the circular area and the cylindrical edge. For MCMBs, because of its sphere-like structure, this type of carbon is able to intercalate lithium ions more uniformly (i.e. 360°). The effect of additives (B, Ag and Sn) in the two carbon samples (CF and MCMB) on the electrochemical performance was also investigated.

Keywords: Carbon fibers; Lithium-ion batteries; Mesocarbon microbeads; Boron-doped carbon fiber

1. Introduction

Many research scientists in the last 20 years have confirmed that carbon materials are a good substitute to metallic lithium as the anode in lithium batteries applications [1]. It is obvious that many carbons exist but only a selected number has the proper characteristics for use in electrochemical systems. For this study, two kinds of carbon materials were chosen because of their interesting properties: the mesocarbon microbeads (MCMBs) and the carbon fibers (CFs). Instead of graphite which have two planes (edge and basal) where intercalation is possible, CFs have single or two-dimension planes available for intercalation. MCMBs have the possibility to intercalate lithium ions all around the microsphere (360°). The purpose of this study is to investigate the effect of heat-treatment (HT) on the carbon structure, and to compare the electrochemical performance and intercalation mechanisms of CFs [2] versus particles. Turbostratic disorder is eliminated by HT [3], and the structure rearranges to that approach the graphite stacking layer planes [4]. The effect of additives in the carbon matrix was also studied (B, Ag and Sn). The additive improves the electrochemical performance, for example, boron-doped CFs, are used to enhance the safety and the electronic conductivity of the lithiated anode. The relation between electrochemistry and the structure is discussed and characterized by XRD, Raman spectroscopy, scanning electron microscopy (SEM) and transmission electron microscopy (TEM).

2. Experimental

The carbon samples were heat-treated in a Labmaster furnace (Thermal Technology Inc.). The precursors were obtain from commercial sources: MCMBs from Kawasaki Steel Corporation and CFs from Petoca Ltd. (Japan). The HTs were done under helium (He) atmosphere for 2 h at different temperatures varying between 650 and 2800 °C at LBL laboratory. The set-up used to test the electrochemical performance of the material is a three-electrode electrolytic cell. The solvent used to make the MCMB and CF slurry was NMP. The carbon material was spread onto a copper grid to avoid adhesion problems, and then dried under vacuum at 95 °C before the electrochemical measurements. A foil of metallic lithium was used as the counter and reference electrodes in a three-electrode cell. The voltage range of 0–2.5 V versus Li/Li^+ was used. A constant current at the *C*/24 rate (15.5 mA/g) was used for both charging and

---

[*] Corresponding author. Tel.: +1-514-652-8019; fax: +1-514-652-8424.
E-mail address: karimz@ireq.ca (K. Zaghib).

0378-7753/02/$ – see front matter
PII: S0378-7753(02)00009-5

discharging the cell. The battery-grade electrolyte solutions were EC:DMC (1:1) $LiClO_4$ (1 M) and EC:DMC (1:1) $LiPF_6$ (1 M) from Tomiyama Pure Chemical Industries Ltd. The half-cells were built in a glove box under an argon atmosphere containing less than 5 ppm of humidity. The temperature in the glove box is controlled at 25 °C. The three-electrode cells were cycled with a MacPile II from Bio Logic (France). Impedance spectrums of each cell are taken before and after cycling with a Solartron SI 1287 electrochemical interface and a Solartron SI 1260 impedance gain-phase analyzer. The surface area was measured with the Quantachrome autosorb automated gas sorption system with nitrogen (N_2). The lattice parameters such as d_{002} spacing, L_a and L_c were obtained from XRD measurements and Raman experiments. The SEM were taken with a high resolution Hitachi SEM (model S4700).

3. Results and discussion

3.1. Changes of the structural parameters of CF and MCMB

The XRD and Raman experiments show a relationship between the heat-treatment temperature (HTT) and the structural parameters for the heat-treated MCMBs and CFs. From Figs. 1 and 2, it is observed that the interlayer spacing d_{002} and L_c varies with the heating temperature; the d_{002} value decreases from 3.51 to 3.37 Å for CF and from 3.54 to 3.38 Å for MCMB, indicating that the dimension and number of carbon layers in a crystallite is increasing. Even if both carbons have a different geometry, the same effect is observed: the interlayer spacing is getting closer to that for the natural graphite interlayer spacing, 3.35 Å, when the

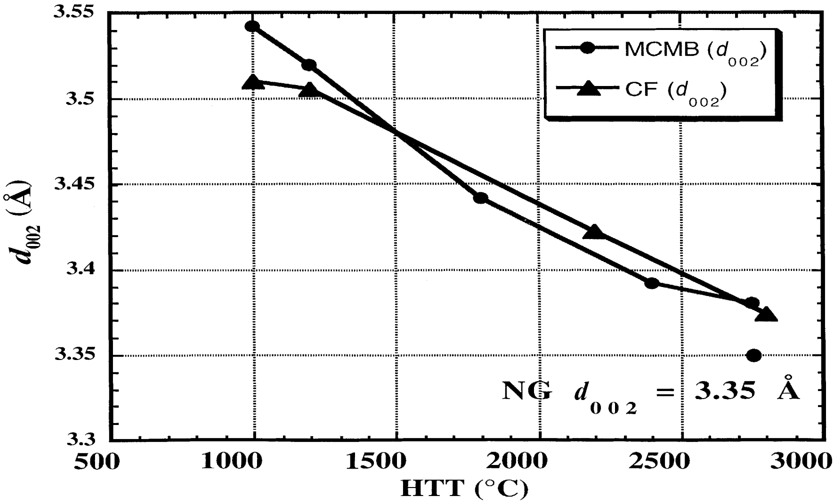

Fig. 1. Variation of interlayer spacing, d_{002} (Å), with the HTT of CF and MCMB.

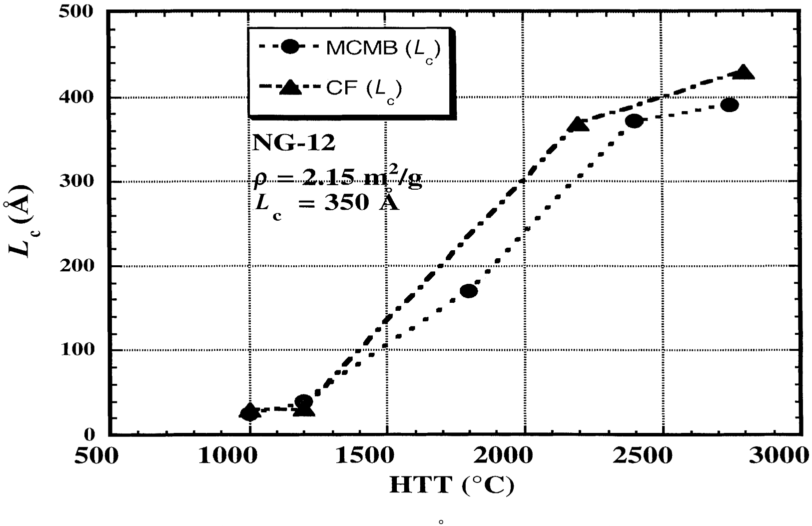

Fig. 2. Variation of the crystallite size, L_c (Å), with the HTT of CF and MCMB.

Table 1
BET surface of heat-treated CF and MCMB

MCMB HTT (°C)	BET surface (m^2/g)	CF HTT (°C)	BET surface (m^2/g)
700	26.94	700	4.56
1000	3.53	1000	1.51
1200	3.43	1200	1.07
1800	4.66	–	–
2400	3.44	2200	0.81
2750	3.85	2800	0.76

HTT is raised. Another effect of HT is the crystallite is the change along the *a*- and *c*-axis. The L_c value increases from 30.0 to 429.7 Å with CF and from 26.0 to 389.7 Å with MCMB. The results of HT from 700 to 2800 °C is an ordering process: along the *c*-axis the carbon layers rearrange to form well-ordered graphite layer planes. The BET surface areas are given in Table 1 for HT CF and MCMB. The BET surface area of CF is small, varying between 1.51 and 0.76 m^2/g after heat treatment at 1000–2800 °C. This result imply that the dimensions of the fiber (diameter and length) do not vary significantly with HT, but the surface area decreases as the HTT increases. The lower surface area is obtained at the highest HTT. The MCMB specific surface area varies from 4.43 and 4.66 m^2/g at HTT of 1000–2750 °C. These results indicate that the particle size is essentially unchanged after HT. The highest BET surface area was obtain with HT at 1800 °C.

3.2. SEM of heat-treated CF and MCMB

The microsphere, which physically characterize the MCMB morphology, is present in the micrographs in Figs. 3–6. The average diameter of the MCMBs and the particle structure are different for the various samples. The sphere-like structure is observed for the MCMB obtained at 700 °C (Fig. 3), but is not as round and regular as the starting material. A comparison of the SEM micrographs of the MCMB HT at 700 °C and HT at 1200 °C (Fig. 4), suggest that the spherical morphology is destroyed at higher HTT. At a HTT of 2400 and 2750 °C (Figs. 5 and 6, respectively), the SEM shows only a very low fraction of microspheres.

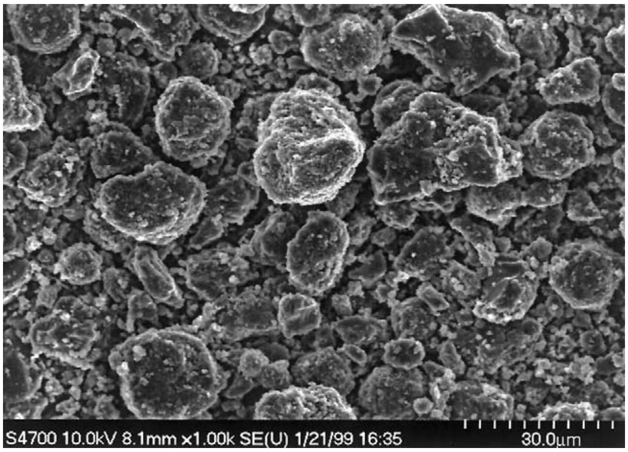

Fig. 3. SEM picture of MCMB heat-treated at 700 °C.

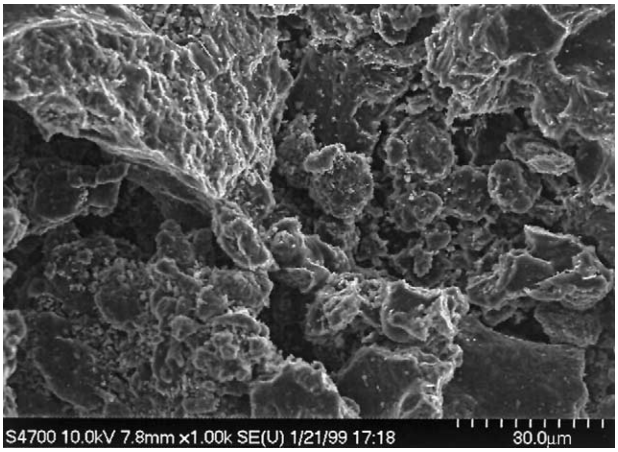

Fig. 4. SEM picture of MCMB heat-treated at 1200 °C.

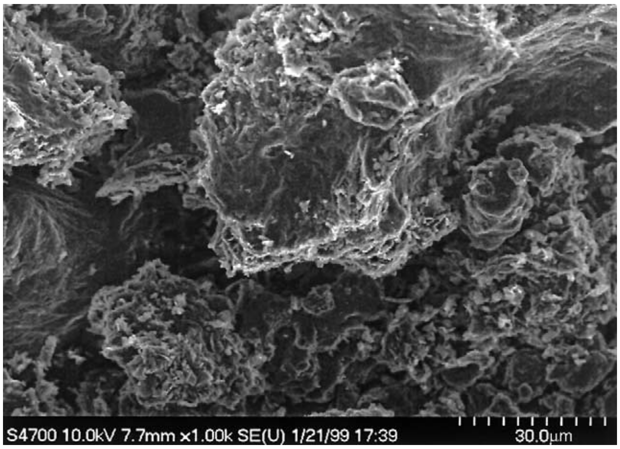

Fig. 5. SEM picture of MCMB heat-treated at 2400 °C.

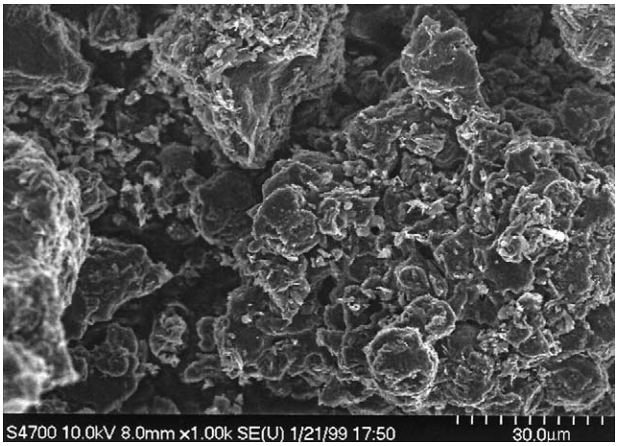

Fig. 6. SEM picture of MCMB heat-treated at 2750 °C.

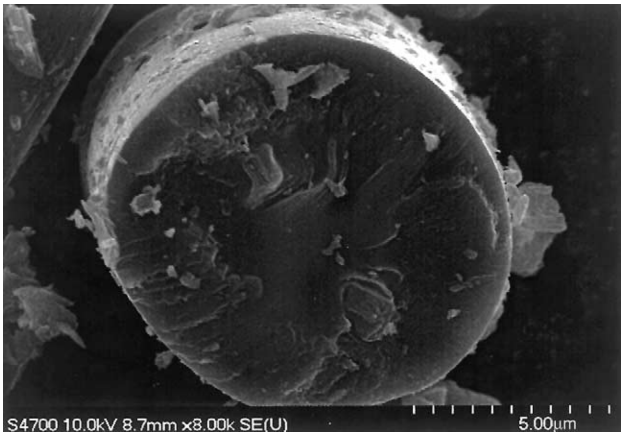

Fig. 7. SEM picture of CF heat-treated at 700 °C.

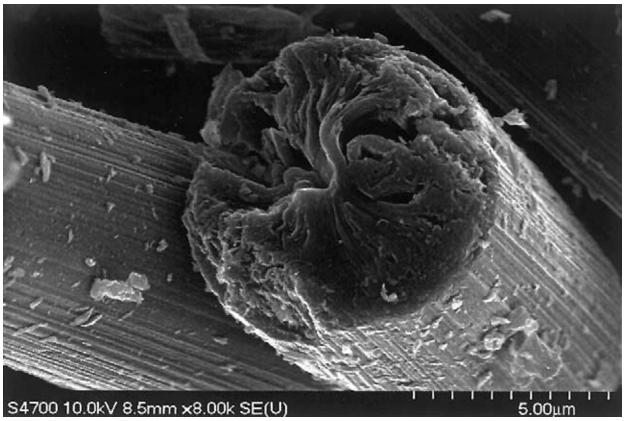

Fig. 9. SEM picture of CF heat-treated at 2200 °C.

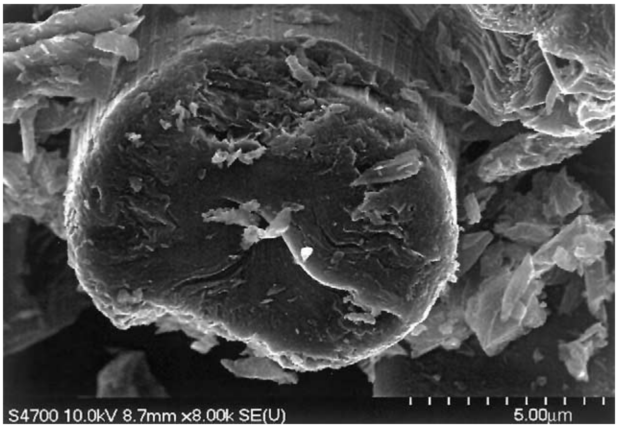

Fig. 8. SEM picture of CF heat-treated at 1200 °C.

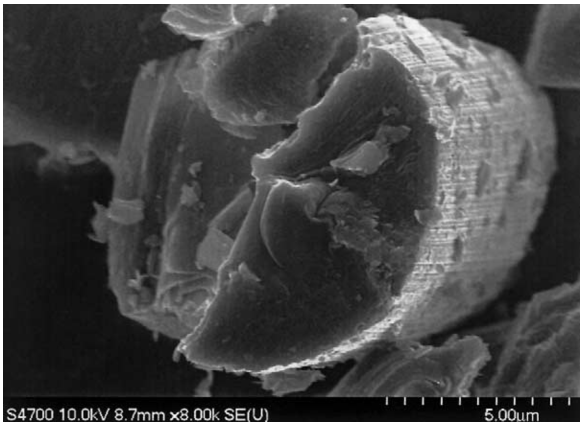

Fig. 10. SEM picture of CF heat-treated at 2750 °C.

However, an increase in HTT increases the order of the carbonaceous structure, thus the capacity to intercalate lithium ions is enhanced. This trend in the crystallographic structure is supported by XRD analysis which shows a shift in the d_{002} spacing from 3.5425 Å (1000 °C) to 3.3803 Å (2750 °C), which is close to that for graphite, i.e. d_{002} spacing of 3.35 Å. The SEM micrographs of HT CF are presented in Figs. 7–10. It is possible to see the surface

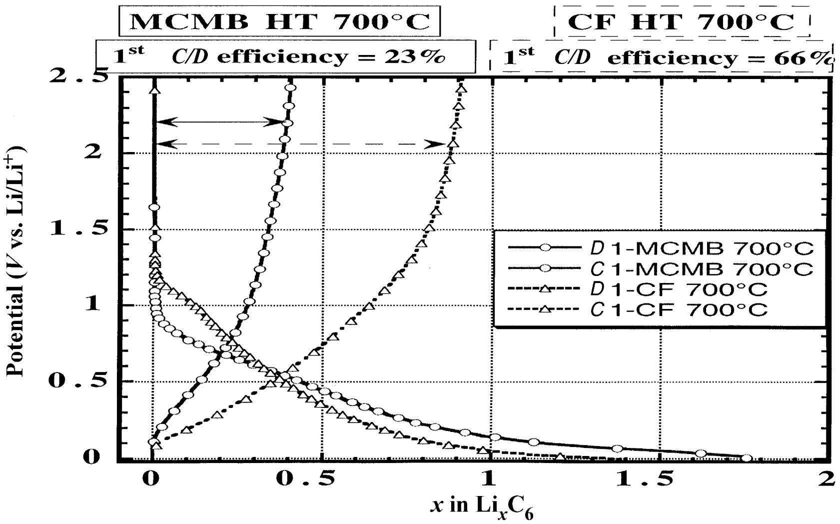

Fig. 11. First discharge–charge cycle of CF and MCMB heat-treated at 700 °C (C/24 rate).

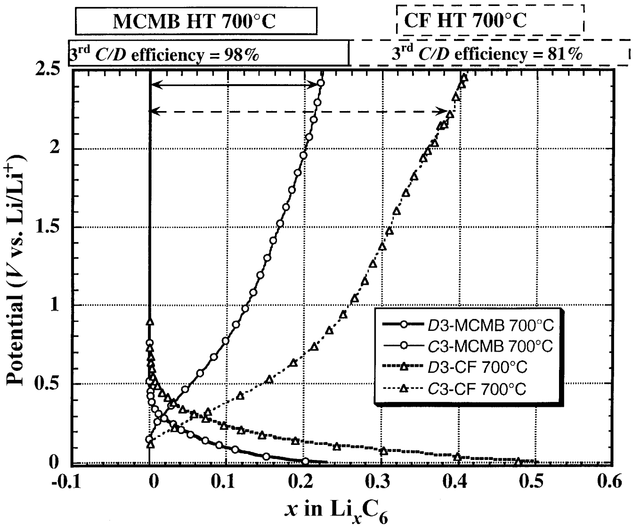

Fig. 12. Third discharge–charge cycle of CF and MCMB heat-treated at 700 °C (C/24 rate).

features on the cylindrical edge of the fibers. The cross-sections of the fibers decrease slightly with an increase in the HTT. The carbon layer planes become more aligned at HTT of 2200 and 2750 °C (Figs. 9 and 10).

3.3. Electrochemical properties of heat-treated CF and MCMB

Fig. 11 show the first discharge–charge curves for CF and MCMB heat-treated at 700 °C. During the first discharge, the electrochemical activity of CF and MCMB begins around 1.2 V and 900 mV versus Li/Li^+, respectively. Both carbons show significant electrochemical activity, indicated by a capacity of 512.2 and 656.6 mAh/g for CF and MCMB, respectively. According to Mabuchi et al. [5], the high discharge capacity for MCMBs obtained at low HTT is due to the large amount of cavities present in the structure. However, the reverse process shows more disparities: only about 66% of the capacity is removed from CF, while only

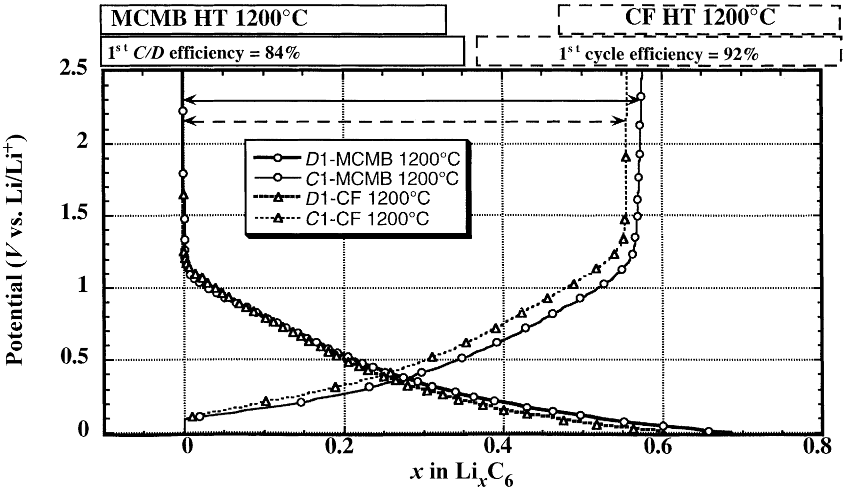

Fig. 13. First discharge–charge cycle of CF and MCMB heat-treated at 1200 °C (C/24 rate).

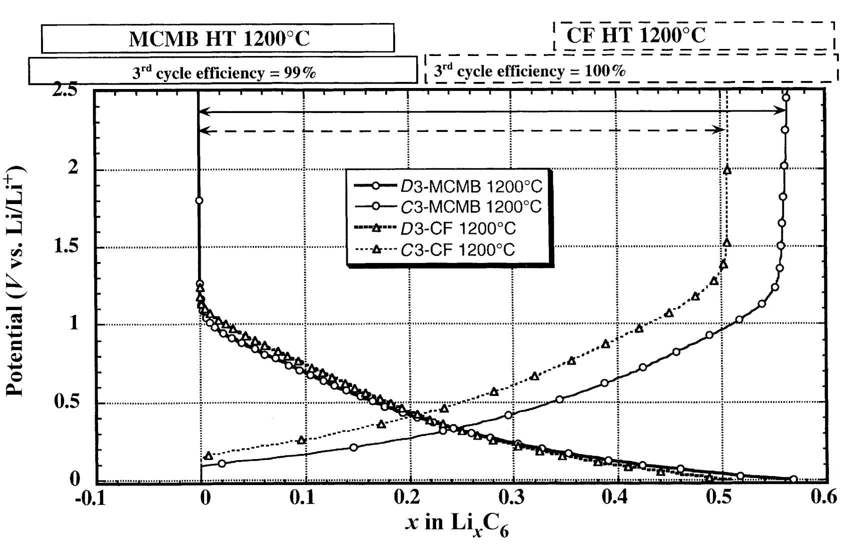

Fig. 14. Third discharge–charge cycle of CF and MCMB heat-treated at 1200 °C (C/24 rate).

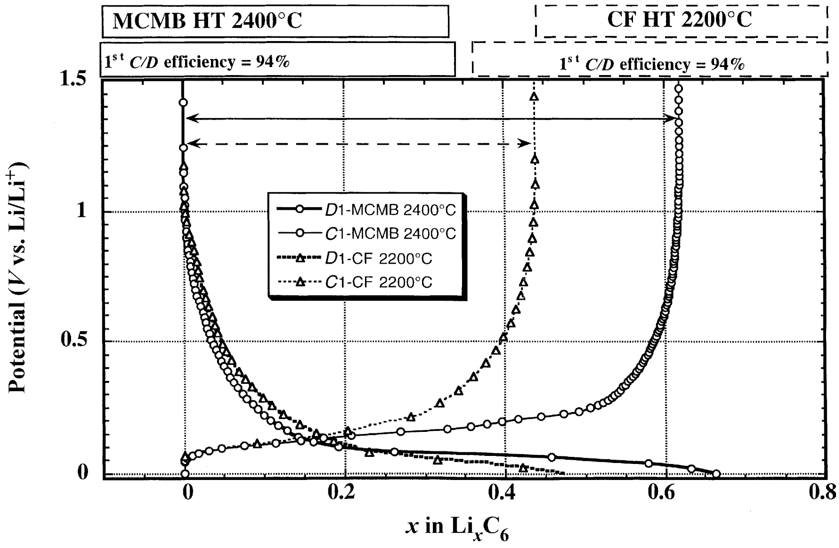

Fig. 15. First discharge–charge cycle of CF heat-treated at 2200 °C and of MCMB heat-treated at 2400 °C (*C*/24 rate).

23% is removed from MCMB. As expected, the irreversible capacity loss (ICL) is more important in the case of MCMB than that with CF. There is probably some cavities present in the CF but the amount should be much lower than that in MCMB. The third cycle of CF and MCMB heat-treated at 700 °C is shown in Fig. 12. The capacity of CF is twice that of MCMB but the efficiency is better for the latter: 98% compared to 81% for CF. The large hysterisis in the plots indicate that the lithium ions inserted in the structure are trapped and difficult to remove.

Fig. 13 illustrate the first discharge–charge cycle of the 1200 °C HT CF and MCMB. The ICL is much less than that observed with the 700 °C HT carbons. The electrochemical activity begins around 1.1 V in both case. The first coulombic efficiency (CE) is still higher for CF (92%) than for MCMB (84%). The large difference between the initial CE at 700 and 1200 °C is explained by the reduction of the amount of cavities present in the carbon structure. Another disparity between HT at 700 and 1200 °C is the elimination of the hysteresis. The third cycle of CF and MCMB HT at 1200 °C both show high CE, near 100% (Fig. 14).

The first discharge–charge curves for CF and MCMB HT at 2200 and 2400 °C are shown in Fig. 15. The MCMB HT at 2400 °C shows the features of graphitized carbon: the intercalation and de-intercalation process occur at potentials <250 mV. The slow cyclic voltammetry (SCV) curve presented in Fig. 16 agrees with the results obtained by constant current cycling; the current–potential peaks caused by the formation of the intercalation staging compounds are clearly observable in the SCV. At >250 mV during charge, no other electrochemical reactions occur at potentials up to 2.5 V. The CF HT at 2200 °C demonstrate the fact that even a 200 °C difference in HTT is important in terms of expansion of the carbon layer planes: an *x* of 0.37 is obtained between

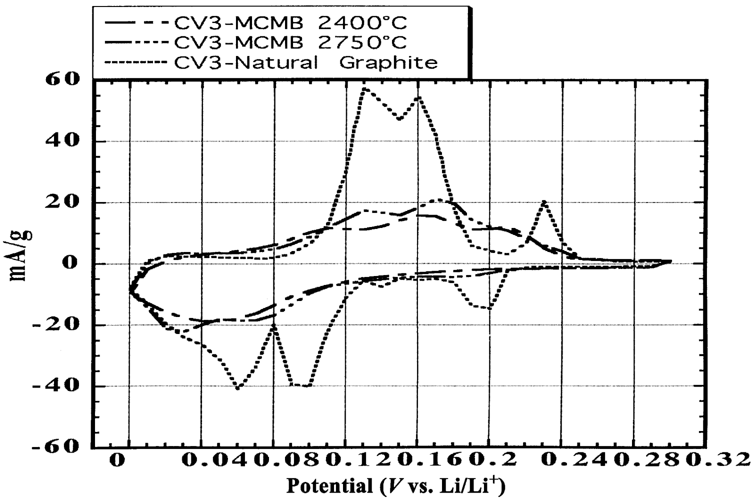

Fig. 16. Slow cyclic voltammetry of 2400 and 2750 °C MCMB vs. NG (SCV was done at a 10 mV/h rate).

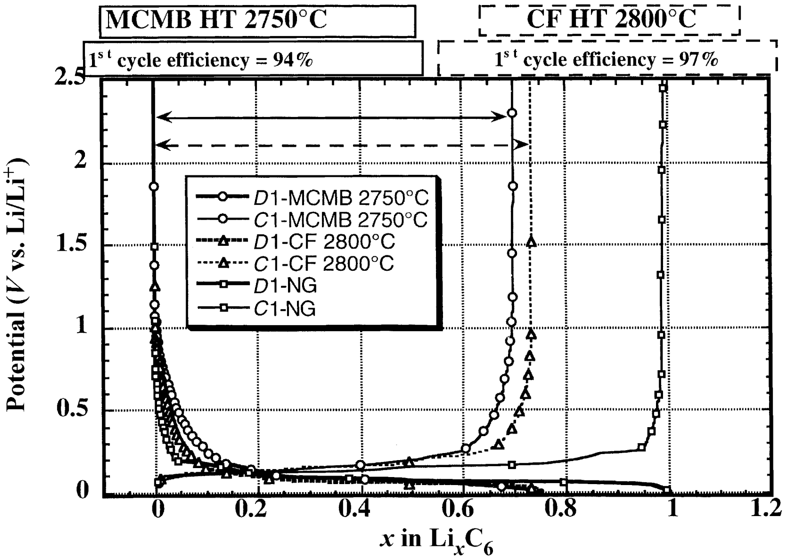

Fig. 17. First discharge–charge cycle of CF heat-treated at 2800 °C and of MCMB heat-treated at 2750 °C.

0.25 and 0 V. For the MCMB HT at 2400 °C, $x = 0.57$: more layer planes are available for the intercalation process to take place. The third cycle shows a completely reversible process which has a nominal efficiency of 100%.

The first cycle for 2800 °C CF and 2750 °C MCMB are plotted in Fig. 17. A remarkably high CE of 97% is obtained with CF HT 2800 °C. The reversible capacity obtain, 272.8 mAh/g, is lower than the theoretical capacity of LiC_6. In both cases, the intercalation plateaus are recorded (see the SCV results in Fig. 16) but the capacity is not higher than 280 mAh/g. This can be explain by the fact that even if most of the cavities, the turbostractic disorder and the unorganized carbon structure were eliminated, there is still some defects in the crystallites.

To further analyze the results, the data for the first and third cycles were separated into four potential regions, OCV to 0.5 V, OCV to 0.25 V, 0.5–0.25 V and 0.25–0 V. The capacities from these regions, x in Li_xC_6, are reported in Table 2. It is obvious that when soft carbons are heat-treated at temperature below 1000 °C, the capacity from OCV to 0.25 V is getting close to LiC_6 (Table 2). It is known that the intercalation mechanism in graphitized carbons occur at potentials below 250 mV. Before this potential, a very small capacity is recorded and is associated to the formation of the passivation layer (SEI). Furthermore, the first discharge capacity of MCMB heat-treated at 700 °C, 656.6 mAh/g, agrees with the fact that the intercalation mechanism is not sufficient to explain the large capacity.

3.4. Electrochemical performances of CF and MCMB at high rate

The capacity of MCMB HT at 2750 °C at a *C*/6 rate is reaching 62% of the capacity that is obtained at a *C*/24 cycling rate. The discharge–charge curve for MCMB is depicted in Fig. 18. This can be partially explained by the fact that the HT procedure used for this study was not optimized. Because the shape of the MCMB particles obtained at a HTT of 2750 °C is not spherical, the particle morphology is not ideal for high diffusion of lithium ions. The results obtained with CF HT at 2800 °C reached 94% of the capacity that is obtained at a *C*/24 cycling rate. Fig. 18 also illustrates the efficiency of CF 2800 °C cycled at a *C*/6 rate. The capacity of CF at *C*/6 rate is 98 mAh/g higher than that of MCMB obtained at the same rate. Thus, CF has the capability to support high cycling rate. This data is supporting by TEM analysis. The image of CF heat-treated at 2750 °C (Fig. 19), the layers of carbon are parallels and

Table 2
First discharge capacities (x in Li_xC_6) of MCMB and CF heat-treated between 700 and 2800 °C

HTT (°C)	OCV to 0.5 V (x in Li_xC_6)	OCV to 0.25 V (x in Li_xC_6)	0.5–0.25 V (x in Li_xC_6)	0.25–0 V (x in Li_xC_6)
700 MCMB	0.437	0.754	0.317	1.009
700 CF	0.385	0.600	0.215	0.779
1200 MCMB	0.213	0.359	0.146	0.325
1200 CF	0.201	0.326	0.125	0.278
2400 MCMB	0.035	0.089	0.054	0.574
2200 CF	0.047	0.112	0.065	0.359
2750 MCMB	0.043	0.101	0.058	0.646
2800 CF	0.025	0.063	0.038	0.695

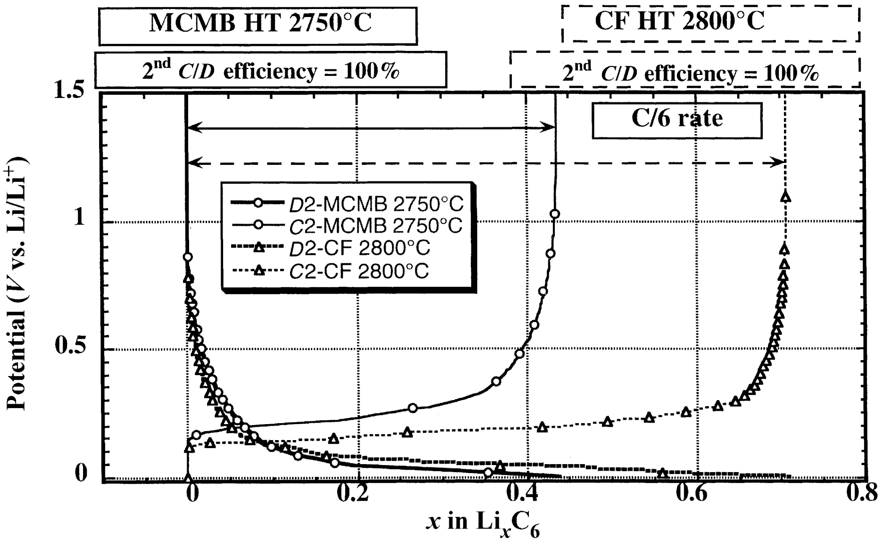

Fig. 18. Discharge–charge curves of CF HT 2800 °C and of MCMB HT 2750 °C (*C*/6 rate).

well organized. For MCMB heat-treated at 2750 °C, the image show (Fig. 20) some vacancy space in the ends of the particle. The parallel arrangement of the layers is not completely uniform.

3.5. *Effect of doping CF and MCMB with B, Ag and Sn*

Tables 3–6 summarize the electrochemical performance (see Figs. 21 and 22) obtained at a *C*/24 cycling rate. It is apparent that the ICL is higher when a metal is added to the electrode because the metal reacts with the electrolyte in an irreversible process. The advantage of a metal on the electrochemical performance is evident during further cycling. The results in Table 3 clearly show that when 10 wt.% Ag and Sn are added to MCMB after HT at 2750 °C, the capacity increases by about 33 mAh/g. This gain in capacity occurs at low potentials (<100 mV) and is attributed to the lithium storage capacity of the metal. At <100 mV, a Li–Ag

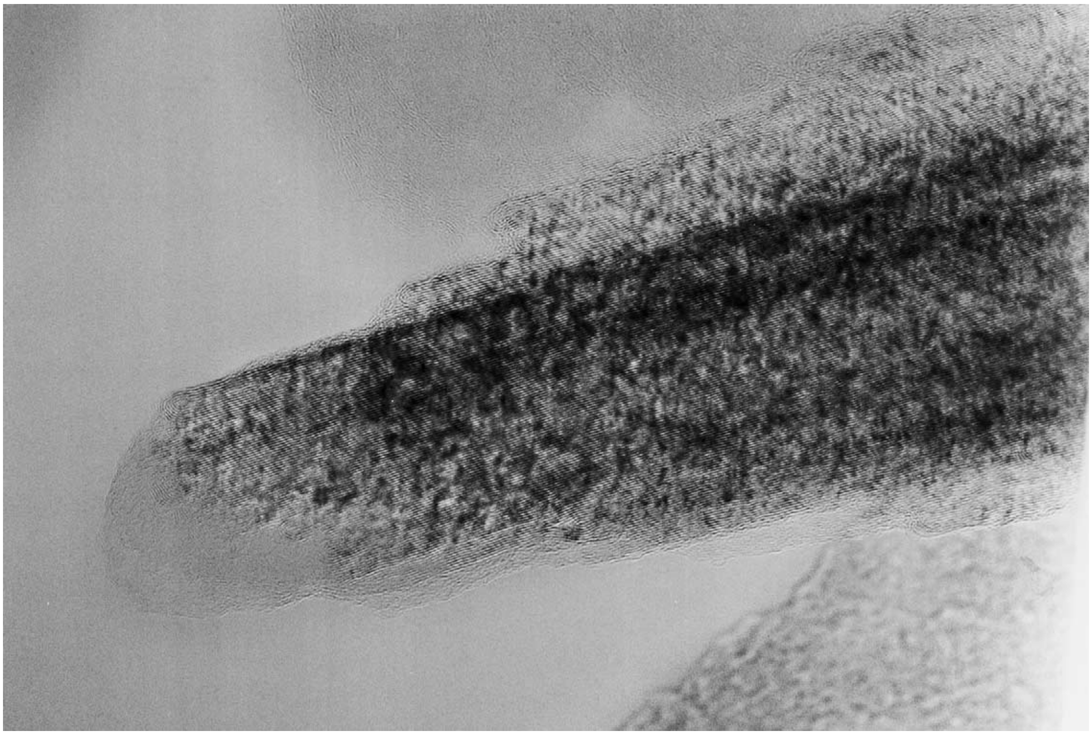

Fig. 19. TEM picture of CF heat-treated at 2750 °C (20 mm=10 nm).

Fig. 20. TEM picture of MCMB heat-treated at 2750 °C (20 mm=10 nm).

Table 3
Electrochemical performances of the first cycle of Ag- and Sn-doped MCMB HT at 2750 °C

Material	D_1 (x)	C_1 (x)	C_1/D_1 (x)	D_1 (mAh/g)	C_1 (mAh/g)	Discharge mean potential (mV)	Charge mean potential (mV)
MCMB 2750 °C	0.747	0.700	94	278.0	260.5	80	156
MCMB 2750 °C + Ag	0.971	0.832	86	361.2	309.5	89	148
MCMB 2750 °C + Sn	1.093	0.859	79	406.6	319.6	93	161

Table 4
Electrochemical performances of the third cycle of Ag- and Sn-doped MCMB HT at 2750 °C

Material	D_3 (x)	C_3 (x)	C_3/D_3 (x)	D_3 (mAh/g)	C_3 (mAh/g)	Discharge mean potential (mV)	Charge mean potential (mV)
MCMB 2750 °C	0.701	0.699	100	261.0	260.1	78	152
MCMB 2750 °C + Ag	0.803	0.789	98	298.7	293.5	81	148
MCMB 2750 °C + Sn	0.805	0.788	98	299.5	293.1	79	158

alloy is formed and this enhances the safety of the electrode. In case of a thermal runaway, the alloy can be beneficial because it has a high melting point. For metal-doped CF, a completely different behavior is found with the Ag and Sn additives. Instead of enhancing the capacity of the third cycle, the capacity is half that of the CF without additive. However, the boron-doped CF gives some interesting results. The B-doped CF has higher capacities, approaching

Table 5
Electrochemical performances of the first cycle of B-, Ag- and Sn-doped CF HT at 2800 °C

Material	D_1 (x)	C_1 (x)	C_1/D_1 (x)	D_1 (mAh/g)	C_1 (mAh/g)	Discharge mean potential (mV)	Charge mean potential (mV)
CF 2800 °C	0.758	0.733	97	282.1	272.8	63	164
B-doped CF	0.931	0.891	96	346.7	331.8	81	155
CF 2800 °C+ Ag	0.853	0.670	79	317.3	249.2	83	158
CF 2800 °C + Sn	0.902	0.675	75	335.5	251.1	97	180

Table 6
Electrochemical performances of the third cycle of B-, Ag- and Sn-doped CF HT at 2800 °C

Material	D_3 (x)	C_3 (x)	C_3/D_3 (x)	D_3 (mAh/g)	C_3 (mAh/g)	Discharge mean potential (mV)	Charge mean potential (mV)
CF 2800 °C	0.729	0.727	100	271.2	270.6	66	168
B-doped CF	0.878	0.874	100	326.9	325.4	74	162
CF 2800 °C + Ag	0.420	0.349	83	156.2	129.8	61	154
CF 2800 °C + Sn	0.470	0.443	94	174.8	164.58	79	157

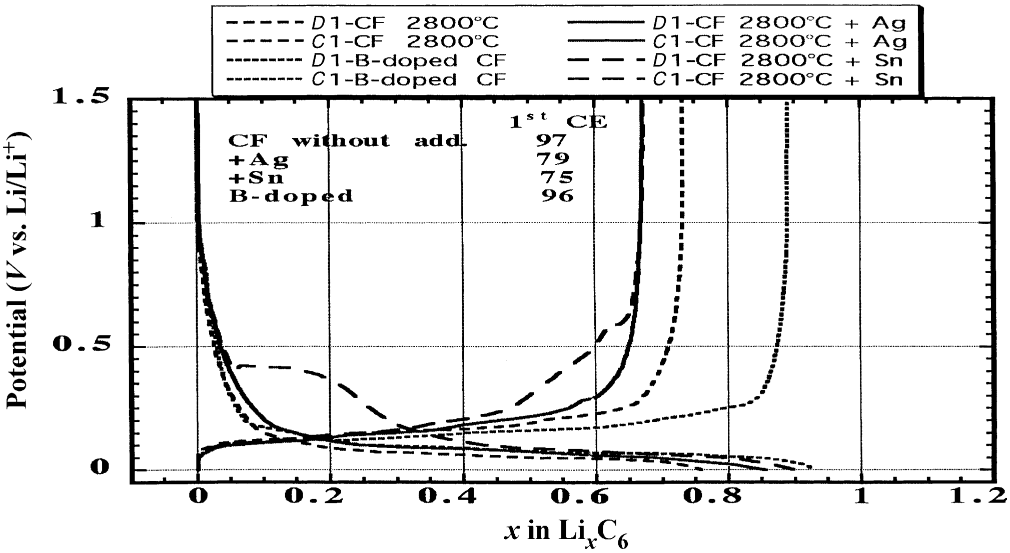

Fig. 21. First cycle of CF HT 2800 °C doped with B, Ag and Sn.

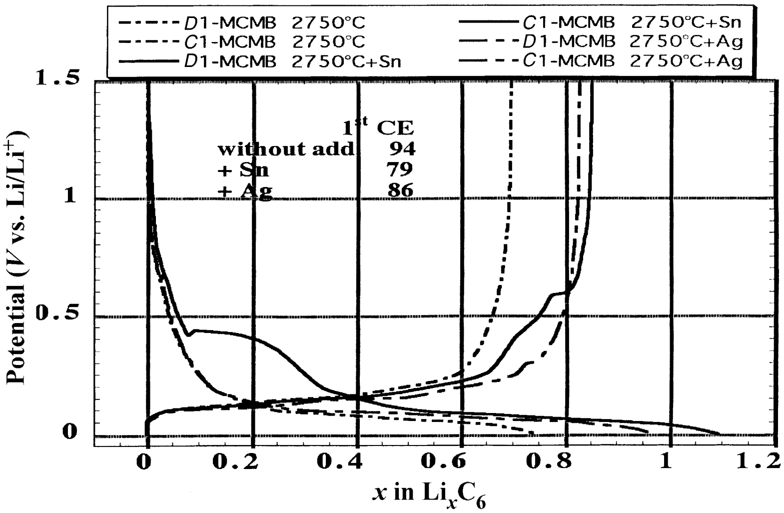

Fig. 22. First cycle of MCMB HT 2750 °C doped with Ag and Sn.

the theoretical value of 372 mAh/g. The boron additive in the CFs matrix plays a significant role in influencing the electrochemical performance. However, more investigations are needed to better understand of the interaction of boron with CF and the electrolyte during the intercalation process.

4. Conclusion

The physical properties of CF and MCMB were modified by HT at 700–2800 °C. The charge–discharge capacities of CF and MCMB tend to decrease as the HTT increases to around 2000 °C and then increases at HTT above 2000 °C. The discharge–charge cycles of CF and MCMB at HTT of 700 °C indicate a difference in the structure of the carbon matrix. At higher HTT, CF and MCMB show almost the same electrochemical behavior and the same capacity. These results suggest that even if the geometry of the carbon materials are quite different, CF and MCMB yield comparable results once they are graphitized. Even if MCMB loose their sphericity during the HT, the carbon layers are able to rearrange to become graphitized. Investigations on the effect of additives were performed. The B-doped CF have a higher capacity than the graphitized CF and approaches the theoretical capacity of natural graphite, 372 mAh/g. Ag- and Sn-doped MCMB HT at 2750 °C are giving higher capacities than MCMB 2750 °C without the additive. In-situ X-ray diffraction will be used in order to identify the mechanism to demonstrate the role of the carbonaceous structure and the metal additive on electrochemical behavior. For the industrial point of view, Boron-doped carbon fiber or graphite by using LiTFSI+$LiBF_4$ in (EC+PC+GBL) is very promising anode for Li-ion gel polymer batteries.

Acknowledgements

The authors would like to acknowledge Hydro-Québec and the US Department of Energy for their financial support. We also want to thanks René Veillette and André Gendron for taking the SEM pictures.

References

[1] Z. Ogumi, M. Inaba, Bull. Chem. Soc. Jpn. 71 (1998) 521–534.

[2] N. Imanishi, H. Kashiwagi, T. Ichikawa, Y. Takeda, O. Yamamoto, M. Inagaki, J. Electrochem. Soc. 140 (1993) 315.

[3] J.R. Dahn et al., Lithium batteries: new materials, developments and perspectives, Ind. Chem. Lib. 5 (1994) 1–47.

[4] H. Shi, J. Barker, M.Y. Saidi, R. Koksbang, J. Electrochem. Soc. 143 (1996) 3466.

[5] A. Mabuchi, K. Tokumitsu, H. Fujimoto, T. Kasuh, J. Electrochem. Soc. 142 (1995) 1041.